Journal of ELECTRONIC MATERIALS, Vol. 44, No. 8, 2015
DOI: 10.1007/s11664-015-3739-z

Effect of Deposition Temperature on the Properties of CdTe Thin Films Prepared by Close-Spaced Sublimation

GUANGGEN ZENG,[1,2] JINGQUAN ZHANG,[1] BING LI,[1] LILI WU,[1] WEI LI,[1] and LIANGHUAN FENG[1]

1.—College of Materials Science and Engineering, Sichuan University, Chengdu 610065, China.
2.—e-mail: yigezeng@sina.com.cn

CdTe films have been prepared by close-spaced sublimation under different conditions. When CdTe is deposited at a low temperature, grains with a single predominant growth plane (111) adhere to the substrate and gather into scattered particles. With increasing deposition temperature, the number of CdTe grains on the substrate increases very quickly, the grains begin to form a quasi-continuous film, and (220), (311), (400), and (331) growth planes of CdTe begin to appear. When the deposition temperature and time are increased further, the CdTe grains begin to accumulate, the pin-holes formed initially begin to disappear, and grain boundaries with traces of layer growth can be observed. Different transmittance of samples of different thickness is clearly apparent but changes of the band gap, E_g, of the CdTe films is negligible. XPS results suggest $CdTeO_3$ is generated on the CdTe film surface as the deposition time is increased.

Key words: Deposition process, close-spaced sublimation, CdTe thin films, solar cell

INTRODUCTION

CdTe with a band gap of 1.46 eV is a direct-band-gap semiconductor material with a high absorption coefficient; a film 1 μm thick can absorb more than 90% of sunlight, and its spectral response is almost identical with the solar spectrum. Because of these advantages, CdTe solar cells have been widely researched in recent years. Because the *p*–*n* junction formed by the *n*-type CdS and the *p*-type CdTe is a crucial component of high-quality CdTe solar cells, CdS and CdTe thin films have been a focus of study for CdTe solar cells.[1–3]

Current research on CdTe focuses on two main aspects, the method of preparation[4–6] and CdTe film treatment.[7–9] High-quality CdTe films can be deposited by a variety of methods, for example close-spaced sublimation (CSS), chemical vapor deposition, screen printing, electron beam deposition, molecular beam epitaxy, sputtering, pulsed laser deposition and electroplating, among others. Because of such obvious advantages as simple equipment, rapid deposition, and low cost, CSS is one of the most popular methods. To obtain high-performance solar cells, the CdTe film must usually be annealed after deposition. Current research on annealing mainly focuses on different annealing methods, selection of different dopants, and the annealing atmosphere.

The temperature difference between source and substrate, the physical mechanism of CdTe sublimation, and the transport and deposition of CdTe thin films deposited by close-spaced sublimation have been reported in our previous paper.[10] However, we did not further investigate growth of the CdTe film throughout the deposition process. Jose studied the deposition rate model for CdTe via close-spaced sublimation spanning the sublimation and diffusion-limited cases and obtained a good quantitative fit with temperature, pressure, and substrate source distance.[11] In addition, growth rates, growth morphology, and film quality for epitaxial CSS CdTe thin films deposited on CdTe (111) B substrates were analyzed over a range of experimental conditions.[12] We showed that deposition temperatures

(Received January 7, 2015; accepted March 6, 2015; published online March 31, 2015)

and time are important factors affecting film deposition. To enable reproducible fabrication of optimum CdTe films of different thickness under different conditions it is, therefore, very important to understand the effect of different deposition temperatures and times on variation of CdTe structure, surface morphology, optical properties, and electronic characteristics. Such analytical instruments as electron microscopes can be used for visual observation of only one plane of the crystal growth process.[13] In this work, a series of CdTe thin films were deposited by using CSS at different temperatures for different times, and scanning electron microscopy (SEM), x-ray diffraction (XRD), ultraviolet–visible spectrophotometry (UV–Vis), and x-ray photoelectron spectroscopy (XPS) were used to study the properties of the polycrystalline thin films of CdTe. The results provide an experimental foundation for preparation of high-quality CdTe films for solar cells.

EXPERIMENTAL

CdTe films were deposited on quartz glass (commercial silica, size $50 \times 60 \times 1$ mm^3, supplied by JNC, China) by use of a laboratory-designed CSS system under a mixed Ar–O_2 atmosphere with O_2 at a partial pressure of 3%. The deposition conditions were: source 99.999% purity CdTe powder, pressure 2 kPa, and distance between substrate and source 2 mm. Deposition temperature and time are listed in Table I.

The CSS process, a physical vapor deposition method, is illustrated in Fig. 1.

When the source temperature reaches 450°C, CdTe on the source will decompose to Cd and Te_2. After several collisions with Ar the Cd and Te_2 are transported to the substrate surface by the O_2 and are uniformly deposited on the surface. Cd and Te_2 have different vapor pressures, which result in different vapor concentrations; as a result, a Te-rich *p*-type CdTe film with a stoichiometry of 1:1.1 can be fabricated by CSS.[14] The deposition process is represented by the equations:

$$\text{The reaction of the source: } 2\text{CdTe (s)} \rightarrow 2\text{Cd (g)} + \text{Te}_2\text{(g)} \quad (1)$$

$$\text{The reaction of the substrate: } 2\text{Cd (g)} + \text{Te}_2\text{(g)} \rightarrow 2\text{CdTe (s)} \quad (2)$$

when the substrate temperature is increased to more than 450°C, CdTe on the surface of the substrate will decompose and sublime just as it does on the source. This process can reduce the amount of CdTe on the substrate. So, to obtain CdTe thin films, one must ensure that the amount of CdTe deposited on the substrate is larger than the amount subliming from the substrate; this can be achieved when the source temperature is higher than the substrate temperature. Figure 2 shows the temperature curve for the deposition process; all samples at different stages during the deposition are marked on the plots.

RESULTS AND DISCUSSION

Figure 3 shows the surface morphology of the samples as revealed by SEM with 10,000× magnification. Film thicknesses measured by use of an SP2 profiler are listed in Table II. When the source temperature is only 470°C and the deposition time

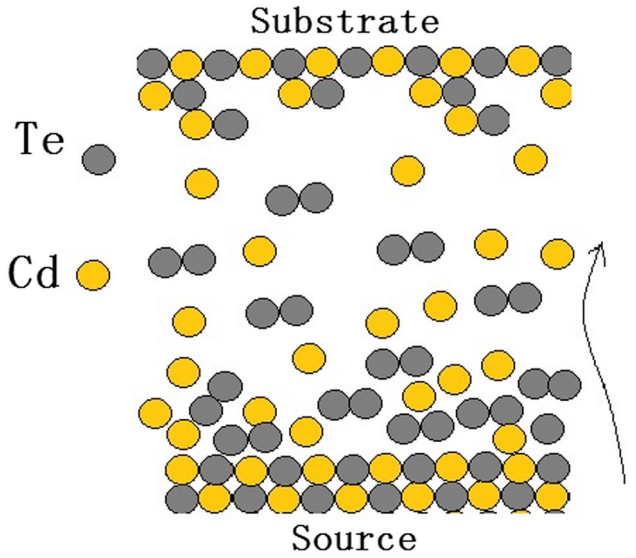

Fig. 1. Process of deposition of a thin film of CdTe by CSS.

Table I. Substrate temperature T_{sub}, source temperature T_s, and the time held at those temperatures for six different CdTe thin films

Sample no.	T_{sub} (°C)	T_s (°C)	Time (min)
1	440	470	0
2	470	520	0
3	500	570	0
4	530	620	0
5	530	620	3
6	530	620	6

is short, no particles could be observed by SEM on sample 1. So, the SEM image for this sample is not shown.

In accordance with the basic equation for the rate of evaporation, R, $R \propto T_s^{-\frac{1}{2}} P_e(T)$ and $\lg(P_e(T)) = A - B/T_s$, where $P_e(T)$, the vapor pressure of the evaporant, is a function of source temperature, A and B are experimental constants. When the deposition temperature exceeds a specific value, a slight increase in the temperature of the source can cause the rate of evaporation to increase rapidly.[15]

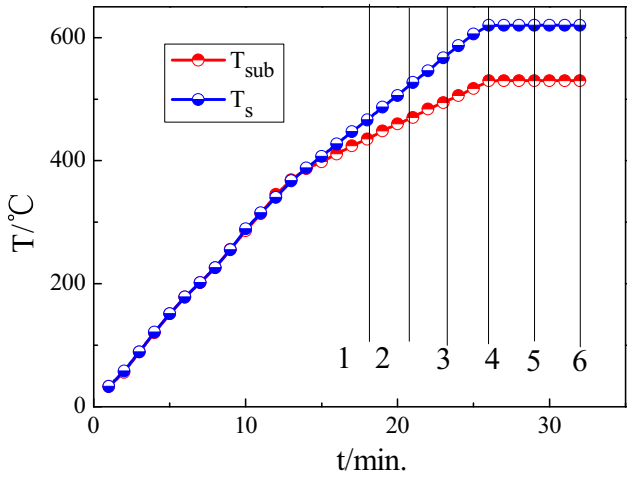

Fig. 2. Substrate temperature T_{sub} and source temperature T_s curves for CdTe during the CSS deposition process.

Although T_s for samples 2, 3, and 4 is increased only slightly, by 50°C, the changes in film thickness and morphology are obvious, as is apparent from Fig. 3 and Table II.

It is apparent from Fig. 3 that at the beginning of CdTe thin film deposition, for example sample 2 (Fig. 3a), isolated and scattered spots of size approximately 0.5 μm become attached to the surface of the glass. As the temperature increases, the grains deposited on the substrate start to grow, filling the gaps and forming a quasi-continuous film. Pin-holes are present between the grains and the size of the grains is approximately 1 μm (Fig. 3b). When the source temperature is increased to 620°C and substrate temperature to 530°C, the grain size increases substantially, to approximately 2 μm (Fig. 3c). Meanwhile, the grain boundaries begin to appear, and differences in grain size becomes large. Compared with sample 3 deposited at a T_s of 570°C and a T_{sub} of 500°C (Fig. 3b), compactness of the film has been improved. For samples 5 and 6 T_s was maintained at 620°C for 3 min (Fig. 3d) and 6 min (Fig. 3e), respectively; fewer smaller grains are present and the uniformity of the film is improved, but clear grain boundaries can be observed with layer growth occurring perpendicular to the direction of the axis along the obvious preferred growth orientation, and the high-index surface becomes smaller or is completely sequestered. Average grain size for sample 6 is >3 μm.

The surface topography of the samples changes for two reasons:

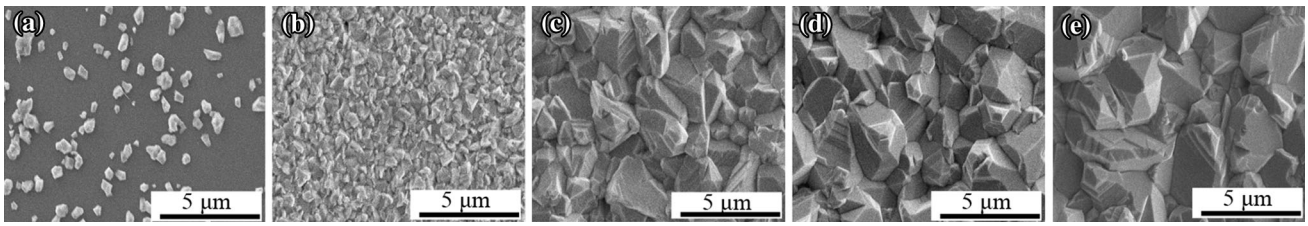

Fig. 3. SEM images of CdTe thin films deposited at different temperatures or time summarized in Table I: (a) sample 2, (b) sample 3, (c) sample 4, (d) sample 5, and (e) sample 6.

Table II. Representative characteristics of CdTe thin films

Sample	Thickness (μm)	Size of SEM image (μm)	E_g (eV)	E_0 (eV)	Intensity of each plane by XRD				
					$I_{(111)}$	$I_{(220)}$	$I_{(311)}$	$I_{(400)}$	$I_{(331)}$
1	–	–	–	–	–	–	–	–	–
2	–	<0.5	–	–	–	–	–	–	–
3	0.4	~1.0	1.485	0.739	1279	688	404	–	–
4	2.9	1.0–2.0	1.492	0.739	4969	1445	1312	293	302
5	4.2	2.0–3.0	1.498	0.738	6175	2259	1736	392	468
6	4.7	~3.0	1.492	0.721	8508	1970	1810	335	483

E_g is the band gap of CdTe, E_0 is the dark conductivity activation energy, I is the intensity of the diffraction peak.

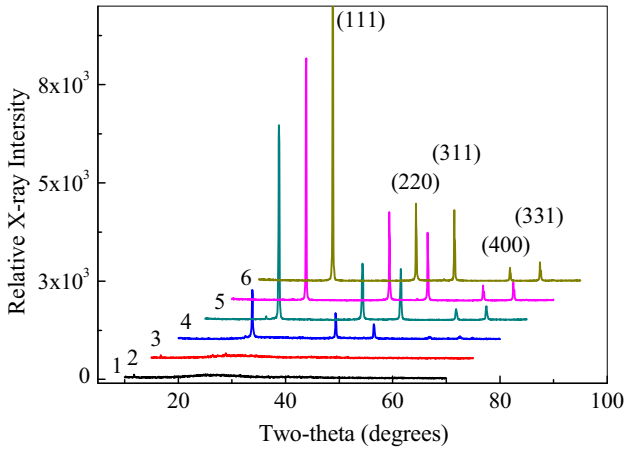

Fig. 4. XRD patterns of CdTe thin films.

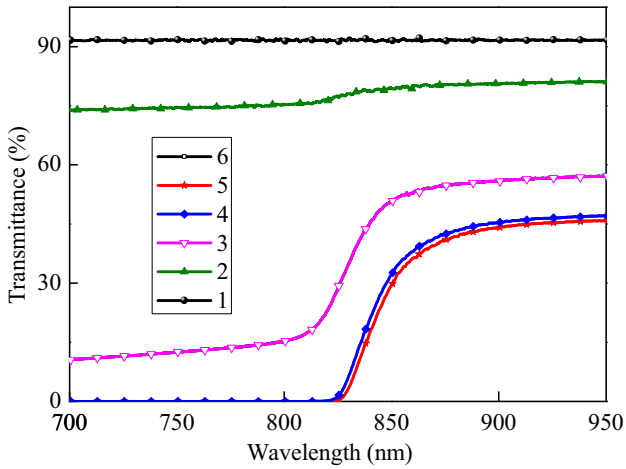

Fig. 5. Transmittance spectra of CdTe thin films.

– First, when the source temperature is increased, the density and kinetic energy of Cd and Te_2 subliming from the source increase. When Cd and Te_2 arrive at the substrate surface, their diffusion velocity becomes faster and the range becomes larger, resulting in an increase in the density of islands on the substrate. This process is very beneficial to growth of the CdTe film.
– Second, the increased substrate temperature improves the thermal vibration of atoms on the surface of the substrate. This process enhances the activity of adsorbed atoms and is conducive to nucleation and growth in a spiral manner, which typically includes adsorption, surface diffusion, and chemical binding on the surface.[16,17]

Temperature and deposition time have a substantial effect on grain shape and size during crystal growth, and preferential growth of the (1 1 1) crystal phase of CdTe can be observed at high substrate temperatures.

XRD diffraction patterns of CdTe films are shown in Fig. 4.

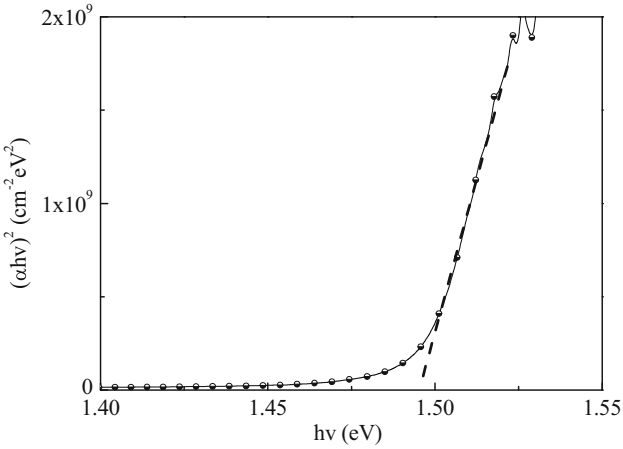

Fig. 6. Typical plot of $(\alpha h\nu)^2$ as a function of $h\nu$ for CdTe thin film.

The XRD curves for samples 1 and 2 are just the amorphous peaks of the substrate, glass, because there is no uniform and continuous CdTe film on the substrate. When deposition temperatures are increased, a continuous CdTe film with a cubic phase begins to grow on the substrate. For the other CdTe films the prevalent preferred orientation plane (111) is apparent. When the deposition temperature is increased to 620°C higher-angle diffraction peaks (56.8°, 62.7°) which are not observed at low temperature begin to appear; these are ascribed to the (400) and (331) crystal planes, respectively. The intensities of the three narrowest and most intense diffraction peaks are listed in Table II; their ratios are:

$$I_{3(111)}/I_{3(220)}/I_{3(311)} = 3.16/1.70/1.00, I_{4(111)}/I_{4(220)}/I_{4(311)} = 3.78/1.10/1.00$$

$$I_{5(111)}/I_{5(220)}/I_{5(311)} = 3.55/1.30/1.00, I_{6(111)}/I_{6(220)}/I_{6(311)} = 4.7/1.08/1.00$$

It is apparent that as deposition temperature and time are increased the preferred orientation (111) crystal plane becomes more obvious; this is confirmed by the increase in the relative intensity ratio from 3.16 to 4.70.[18] This result indicates that crystallinity has improved and no phase transition occurs as the deposition temperature is increased.

The transmittance of the CdTe thin films was investigated by UV–Vis spectroscopy. According to Fig. 5, transmittance (T) depends on the deposition process. T for samples 1 and 2 is very high, especially that for sample 1. T for sample 1 is that of the glass substrate. Because of the presence of black particles on sample 2, T decreases, but remains above 74%. T for the other samples decreases substantially. Sample 3 (0.4 μm) absorbs most of the light below 830 nm, and sample 4 (2.9 μm) absorbs

all the light below 830 nm, because of the continuous, compact, and thicker CdTe films. Substantial overlap is observed for samples 5 and 6. The results indicate that the thickness of CdTe film can be reduced to below 2 μm by controlling the deposition conditions.

It is also apparent from Fig. 5 that the change in T for each sample is almost at the same position, which corresponds to the band gap (E_g) of CdTe. E_g can be calculated by use of the Tauc formula:

$$\alpha h\upsilon = A(h\upsilon - E_g)^n, \quad (3)$$

where $h\upsilon$ is the photon energy, A is a constant, and the value of n depends on the energy band structure of the material. For direct energy band semiconductor material, for example CdTe, $n = 0.5$. Figure 6 shows a typical plot of $(\alpha h\upsilon)^2$ as a function of $h\upsilon$. The linear fit to the straight line part of this plot gives the value of the E_g from the x-axis intercept. The band gaps for samples 3–6 are listed in Table II. The change of E_g for films prepared by use of different temperatures and times is negligible, and E_g is very close to the theoretical value of 1.5 eV.

The room temperature conductivity (σ_0) and dark conductivity activation energy (E_0) are obtained by measuring the conductivities (σ) of the films as a function of temperature. The electron affinity of CdTe is 4.28 eV, so the work function (>5.6 eV) is higher than for most metals. Thus, CdTe is in direct contact with the metal, which produces a Schottky junction resulting in an increase of the contact resistance. To minimize the effect of the contact barrier, Au (work function: 5.1 eV) has been deposited as a co-planar electrode on top of the CdTe. Furthermore, changes of dark resistance as a function of temperature were measured and the dark conductivity (σ) was calculated. Figure 7 shows the relationship between ln (σ) and 1000/T.

For CdTe polycrystalline film, E_0 is calculated by use of the formula $\sigma_{dark} = \sigma_0 e^{E_0/KT}$; the results are listed in Table II:

E_0 is slightly higher for CdTe deposited at a low temperature for a short time than for that deposited at a high temperature for a long time. It is known that E_0 is composed of Fermi energy and activation energy of carrier mobility. CdTe is a unipolar semiconductor with a large number density of defects, because of Cd vacancies and Te interstitials, so it is difficult to change the Fermi energy level because of Fermi-level pinning. The results show that all E_0 are almost half the band gap, which means that both the Fermi energy and activation energy of carrier mobility are independent of deposition temperature and time, even if the defect concentration changes with increasing deposition temperature and time. Annealing is an effective way of reducing E_0 for CdTe thin films.[19,20]

The elemental composition of CdTe was determined by XPS (XSAM-800) with Al Kα radiation under UHV and operating at 12 kV and 12 mA. All the binding energy is referenced to the signal for adventitious carbon at 284.4 eV. Figure 8 shows the binding energies of the Te and Cd levels on the surface of CdTe. The Te peaks are split into doublets.

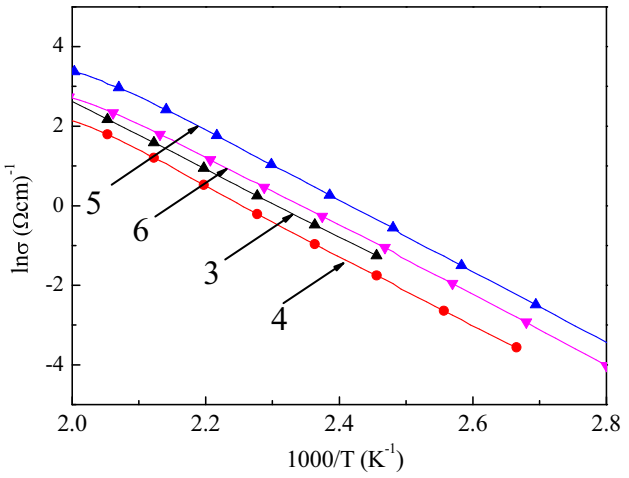

Fig. 7. ln (σ) versus 1000/T curves of CdTe deposited at different temperatures and times.

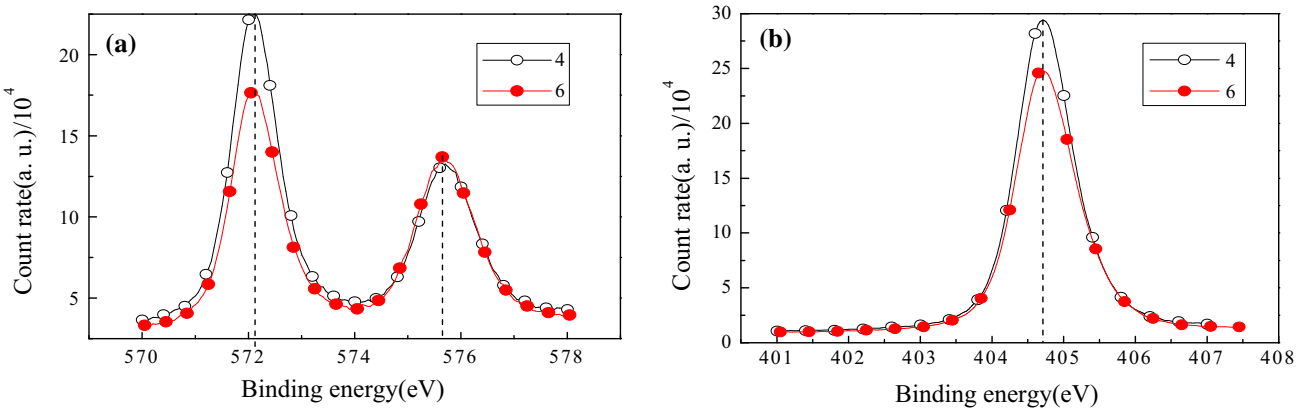

Fig. 8. Photoemission spectra of (a) Te (3d) and (b) Cd (3d) levels for CdTe samples 4 and 6.

The Te $3d_{5/2}$ peak at 572.1 eV corresponds to the Te–Cd bond and the Te $3d_{5/2}$ peak at 575.6 eV corresponds to the Te–O bond (Fig. 8a). With increasing deposition time, the $Te_{572.1\ eV}$ peak area changes. We can estimate the relative change of different bonds by considering the area under each sample. The area ratio $A_{Te,\ 572.1\ eV}/A_{Te,\ 575.6\ eV}$ decreases from sample 4 to 6, which indicates that the Te oxidation state increases in the film and this oxide corresponds to $CdTeO_3$. The Cd peaks (Fig. 8b) with binding energy of 404.7 eV are characteristic of Cd $3d_{5/2}$.

Although we increased the deposition time there was no significant energy shift for Cd, which means there was no change in the chemical state of Cd when CdTe is oxidized to form $CdTeO_3$ because of the Cd^{2+}.[21–23]

CONCLUSIONS

The properties of CdTe thin films prepared at different temperatures and for different times were studied. We found that temperature and deposition time have substantial effects on grain shape and size during crystal growth. When CdTe was deposited at low temperature, isolated, scattered, and small CdTe formations, only, became attached to the surface of the glass, and preferred orientation in the (111) plane could not be observed. Transmittance was substantially affected by film thickness. As the temperature was increased, grains deposited on the substrate began to grow and fill the gaps between each other, and then gradually formed a continuous film. As a result, clear grain boundaries and five narrower and more intense diffraction peaks could be observed, indicating that crystallinity has been improved. It is worth noting that the band gap, dark conductivity activation energy, and structure of CdTe did not change with increasing deposition temperature. However, when the sample was deposited at high temperature for a long time Te oxide was generated on the surface.

ACKNOWLEDGEMENTS

This work was supported by Sichuan Province Science and Technology Support Program (2013 GZX0145). The authors are also very grateful for CSC funding. We wish to thank the Analytical and Testing Center of Sichuan University for XPS measurements.

REFERENCES

1. W. Xuanzhi, *Sol. Energy* 77, 803 (2004).
2. M.A. Green, K. Emery, Y. Hishikawa, W. Warta, and E.D. Dunlop, *Prog. Photovolt. Res. Appl.* 22, 1 (2014).
3. O. Toma, L. Ion, M. Girtan, and S. Antohe, *Sol. Energy* 108, 51 (2014).
4. V.M. Nikale, S.S. Shinde, C.H. Bhosale, and K.Y. Rajpure, *J. Semicond.* 31, 033001 (2011).
5. B. Li, J. Liu, X. Xu, R. Lu, L. Feng, and J. Wu, *Appl. Phys. Lett.* 101, 153903 (2012).
6. W.A. Pinheiro, V.D. Falcão, L.R.O. de Cruz, and C.L. Ferreira, *Mater. Res.* 9, 47 (2006).
7. J.D. Major, R.E. Treharne, L.J. Phillips, and K. Durose, *Nature.* 511, 334 (2014).
8. A. Rios-Flores, O. Ares, J.M. Camacho, V. Rejon, and J.L. Pena, *Sol. Energy* 86, 780 (2012).
9. L. Kranz, C. Gretener, J. Perrenoud, et al., *Nat. Commun.* 4, 2306 (2013).
10. Z. Huajing, Z. Jingquan, F. Lianghuan, Z. Jiagui, C. Wei, L. Bing, and C. Yaping, *J Wuhan Univ. Technol.* 21, 65 (2006).
11. J.L. Cruz-Campa and D. Zubia, *Sol. Energy Mater. Sol. Cells* 93, 15 (2009).
12. A. Escobedo, S. Quinones, M. Adame, J. McClure, D. Zubia, and G. Brill, *J. Electron. Mater.* 39, 400 (2010).
13. S.A. Quiñones, S.M. Ammu, A. Escobedo, et al., *J. Mater. Sci.* 18, 1085 (2007).
14. C.S. Ferekides, D. Marinskiy, V. Viswanathan, B. Tetali, V. Palekis, P. Selvaraj, and D.L. More, *Thin Solid Films* 361–362, 520 (2000).
15. E. Chen, *Appl. Phys.* 298r, 4 (2004).
16. Z. Zhang and M.G. Lagally, *Science* 276, 377 (1997).
17. J.A. Venables, G.D.T. Spiller, and M. Hanbucken, *Rep. Prog. Phys.* 47, 399 (1984).
18. S. Neretina, Q. Zhang, R.A. Hughes, J.F. Britten, N.V. Sochinskii, J.S. Preston, and P. Mascher, *J. Electron. Mater.* 35, 1224 (2006).
19. L. Feng, J. Zhang, B. Li, et al., *Thin Solid Films* 491, 104 (2005).
20. L.L. Wu, L.H. Feng, W. Cai, J.Q. Zhang, Y.P. Cai, J.G. Zheng, J.M. Zhu, and N.F. Chen, *Chin. J. Semicond.* 24, 827 (2003).
21. D.N. Bose, M.S. Hedge, S. Basu, and K.C. Mandal, *Semicond. Sci. Technol.* 4, 866 (1989).
22. B.J. Kowalski, B.A. Orłowski, and J. Ghijsen, *Surf. Sci.* 412, 544 (1998).
23. P. Bartolo-Pérez, R. Castro-Rodríguez, F. Caballero-Briones, W. Cauich, J.L. Peña, and M.H. Farias, *Surf. Coat. Technol.* 155, 16 (2002).